

Mechanism of Oxide Film Destruction in Flux-Free Brazing of Aluminum under an Inert Atmosphere*

Tomoki Yamayoshi**, Yasunaga Itoh*** and Atsushi Fukumoto****

The addition of magnesium or lithium to aluminum brazing sheets was investigated with the aim of the clarifying the mechanism of oxide film destruction during flux-free brazing. The surface of the filler alloy after brazing was observed by scanning and transmission electron microscopy. The presence of complex oxide particles of magnesium or lithium with aluminum were confirmed on the surface of the filler alloy after brazing. The results indicate that the oxide film was broken into oxide particles by magnesium or lithium during brazing, and a new surface of molten filler alloy was exposed between the oxide particles, allowing flux-free brazing.

Keywords: fluxless brazing, flux-free, oxide film, morphology of the surface after brazing

1. Introduction

Aluminum automotive heat exchangers are generally manufactured by brazing. In order to braze aluminum, it is necessary to destroy a strong and stable oxide film present on the material surface. For this reason, methods using a flux or heating in vacuum without using flux have been developed. Currently Controlled Atmosphere Brazing (CAB), destroying the oxide film by using a non-corrosive flux, is a mainstream method. However, it requires flux-free brazing in an inert atmosphere since flux residue in the heat exchanger can become a cleanliness problem.

Materials with added magnesium are known to be brazable without flux in an inert atmosphere. Also, it is reported that flux-free brazeability is improved by adding a wetting element such as bismuth^{1),2)}. A brazing sheet with lithium has also been developed³⁾. Magnesium and lithium added in the flux-free material have lower oxide formation free energy than aluminum. Therefore, it is assumed that these elements destroy the oxide film (Al_2O_3) by a reduction reaction. However, research on the nature of the oxide film after brazing does not seem to have been

investigated.

In this study, the oxide film after brazing of the material containing added magnesium or lithium was observed by Scanning Electron Microscopy (SEM) and Transmission Electron Microscopy (TEM) to clarify the mechanism of oxide film destruction.

2. Experimental procedure

2.1 Materials

Table 1 shows the chemical composition of the brazing sheet provided in this study. As the base composition, the filler alloy contained 10mass% of silicon, and the core alloy contained 1.2mass% of manganese. For No.1 material 0.6mass% of magnesium was added to the filler alloy and for No.2 material 0.6mass% of magnesium was added to the

Table 1 Chemical composition of the brazing sheets. (mass%)

No.	Filler alloy					Core alloy			Remarks
	Si	Fe	Mg	Li	Bi	Cu	Mn	Mg	
1	10	0.17	0.61	-	0.02	0.16	1.2	-	
2	10	0.17	-	-	0.02	0.16	1.2	0.62	
3	10	0.17	-	0.02	0.02	0.16	1.2	-	
4	10	0.17	-	-	-	0.16	1.2	-	Flux application 3 g/m ²

* The definitive version of this article is published in the VTMS13: Vehicle Thermal Management Systems, Institution of Mechanical Engineers, 2017

** Research Department V, Research & Development Division, UACJ Corporation

*** Research Department VII, Research & Development Division, UACJ Corporation

**** Research Department IV, Research and Development Division, UACJ Corporation

core alloy. The No.3 material contained 0.02mass% of lithium in the filler alloy. In order to improve brazeability, for No.1 to No.3 materials 0.02mass% of bismuths was added in the filler alloys. The No.4 material was a comparative material having no added magnesium and lithium, and had a flux of 3 g/m² applied before brazing.

For producing these brazing sheets, the filler alloy was cladded on one side of the core alloy by hot rolling, being rolled down to a thickness of 0.4 mm. The temper is O (annealed), and the cladding ratio of the filler alloy was 10%. The brazing sheets were then degreased with acetone. Finally, the oxide film formed during manufacturing the material was removed by dipping in 2% nitric acid-1% hydrofluoric acid at room temperature for 90 seconds.

2.2 Brazing conditions

Fig. 1 shows the clearance filling specimen used for evaluating the brazeability. For the clearance filling specimen, a vertical plate of 3003 alloy was positioned on a flat brazing sheet, while one end of the plate was raised on a stainless steel rod to provide clearance between the plate and the sheet. **Fig. 2** shows the heating profile. Brazing was performed in a nitrogen gas atmosphere having an oxygen content of 5 ppm

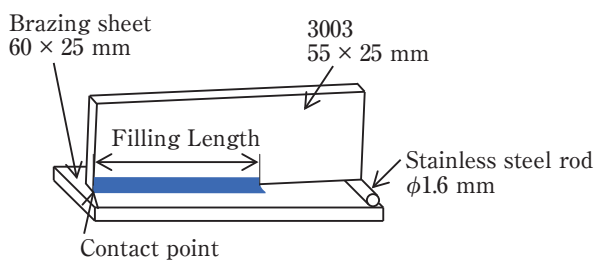


Fig. 1 Schematic of clearance filling specimen.

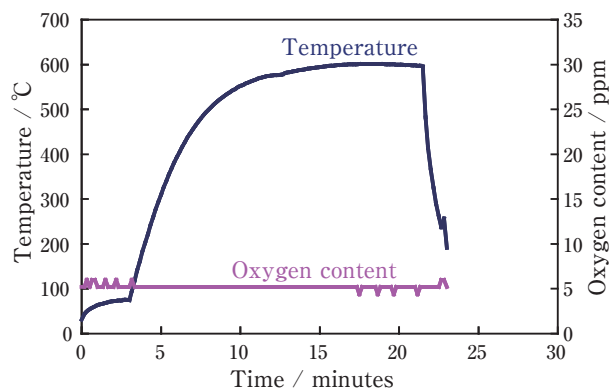


Fig. 2 Heating profile.

or less and a dew point of -70°C or less, and the specimen temperature was held at 597 to 600°C for 5 minutes. After brazing, the specimen was rapidly cooled to 300°C in a nitrogen gas atmosphere having an oxygen content of 5 ppm or less to prevent oxidation during cooling.

2.3 SEM observation and TEM Analysis

To provide specimens of the filled clearance after brazing, the brazing sheets were cut out and the surfaces of the filler alloy were observed by SEM. In addition, the oxide film on the filler alloy after brazing was analyzed by TEM-energy dispersive X-ray spectrometry (EDX). Since lithium is a light element, it can not be detected with EDX. Therefore, lithium was analyzed by TEM-electron energy loss spectroscopy (EELS). A sample for TEM analysis was prepared by dipping the brazing sheet in a saturated iodine methanol solution, leaving only the oxide film.

3. Results and discussion

3.1 Brazing test results

Fig. 3 shows the results of the clearance filling test. No.1 to 3 materials formed a fillet even without flux. The filling length of the brazing sheet containing magnesium in the core alloy (No.2), at 31 mm, was longer than that in the filler alloy (No.1), at 21 mm. However, it was not as large as the filling length using the CAB method (No.4, 38 mm). On the other hand, the material containing lithium in filler alloy (No.3) had a filling length of 36 mm which is comparable to

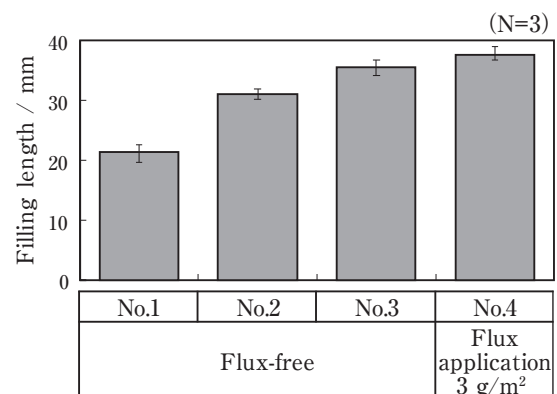


Fig. 3 Results of the clearance filling test.

that of the CAB method. Furthermore, as shown in **Fig. 4**, the No.3 material formed a uniform fillet, which was equivalent to the CAB method. Cross-sections at a position 5 mm from the contact point are shown in **Fig. 5**. All the specimens had a fillet shape essentially identical to that of the CAB method. These results indicate that lithium is an effective element for improving the flux-free brazeability.

3.2 SEM observations

Fig. 6 shows the secondary electron images of the filler alloy surface after brazing for materials No.1 to No.3 and the surface of a representative sample before brazing for material No.1. Fine particles with white or grey contrast were observed on all brazed filler alloy surfaces, and the size of the particles was about 50 to 200 nm. It appears that the oxide film was broken into fine particles during brazing. In addition, a black region with smooth low contrast was

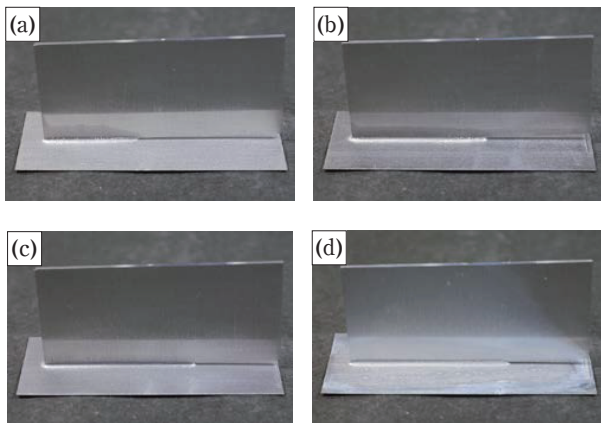


Fig. 4 Appearances of the clearance filling specimens. (a) No.1, (b) No.2, (c) No.3 and (d) No.4 (with flux).

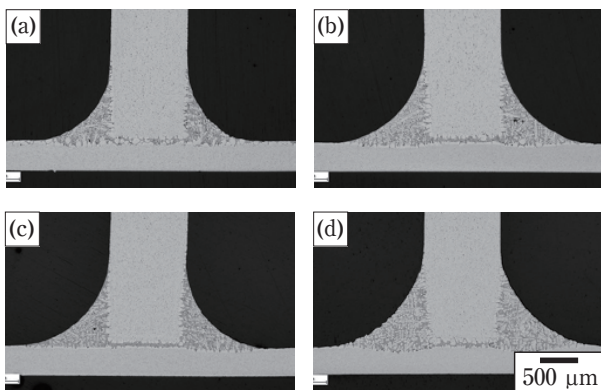


Fig. 5 Cross-sections of the clearance filling specimens at 5 mm from the contact point. (a) No.1, (b) No.2, (c) No.3 and (d) No.4 (with flux).

observed between the fine particles. The area ratio of this black region was obtained by image analysis for the low magnification image shown in **Fig. 7**. Brazing sheet containing magnesium in the filler alloy (No.1) had a black area ratio of only 13%. However, brazing sheet containing magnesium in the core alloy (No.2) had a ratio of 48%. The highest black area ratio was brazing sheet containing lithium in the filler alloy (No.3), which was 67%. The material with good brazeability had a high black area ratio. From this result, it was presumed that the black region is the part where the new surface of molten filler alloy is exposed. Based on these SEM observation results, we surmise that the oxide film was broken into fine particles, and then the new surface of the molten filler alloy was exposed between the particles.

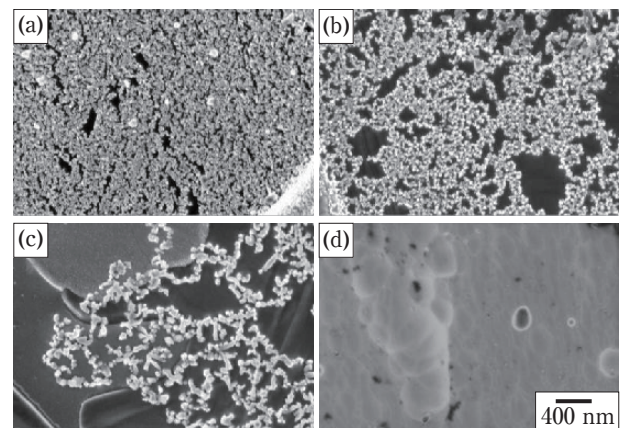


Fig. 6 Secondary electron images of the filler alloy surface (a) No.1, (b) No.2, (c) No.3 after brazing and (d) the surface of a representative sample of material No.1 before brazing (high magnification).

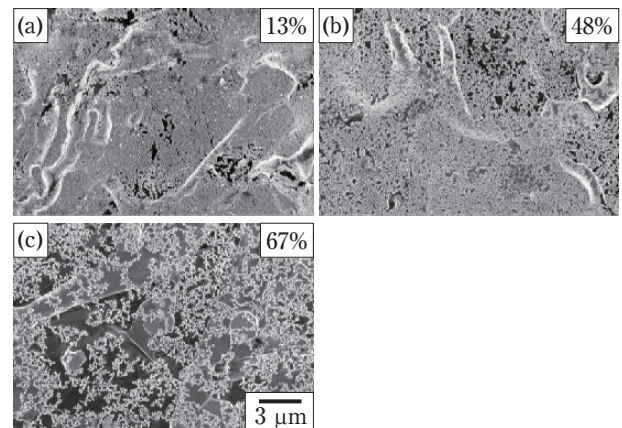


Fig. 7 Secondary electron images of the filler alloy surface after brazing (low magnification) and black area ratio, (a) No.1, (b) No.2 and (c) No.3.

3.3 TEM analysis

TEM analysis was carried out to identify particles observed in the SEM for No.2 and No.3 materials with good brazeability.

Fig. 8 shows the TEM-EDX analyses of particles on the surface of No.2 material after brazing. The particles were observed with black contrast in the TEM image. Aluminium, magnesium, oxygen were detected from all particles. From the diffraction pattern shown in **Fig. 9**, these particles were identified as $MgAl_2O_4$. Note that MgO was not found in this analysis.

Fig. 10 shows the TEM-EELS analysis of particles on the surface of No.3 material after brazing. The particle was observed with white contrast in the STEM image. A strong lithium signal was detected from the particle. Aluminum was detected from around the particle and was also detected in it. In the aluminum region of the spectrum, two peaks were clearly observed. These peaks do not appear if aluminum is a metal, but are characteristic of an oxide. We concluded that lithium-aluminum based oxide particles are formed on the filler alloy surface of No.3 material after brazing.

We thermodynamically verified the validity of observations of a complex oxide with aluminum after brazing. The reaction formula of magnesium or lithium and Al_2O_3 are shown in **Table 2**. Although all

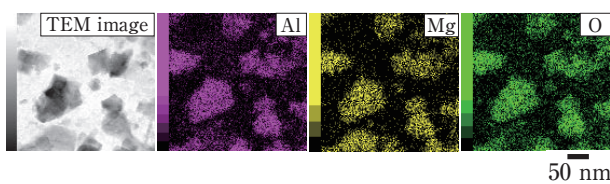


Fig. 8 TEM-EDX analysis of the particles on the surface of No.2 material after brazing.

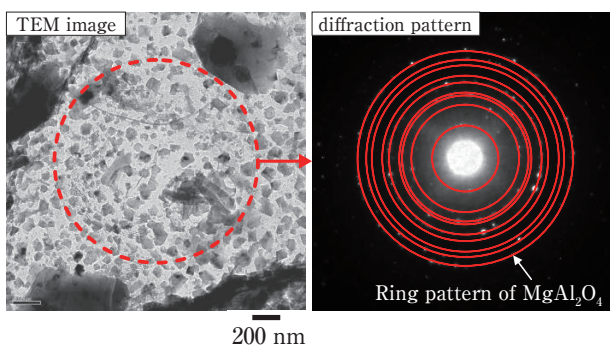


Fig. 9 TEM image and the diffraction pattern of the particles on the surface of No.2 material after brazing.

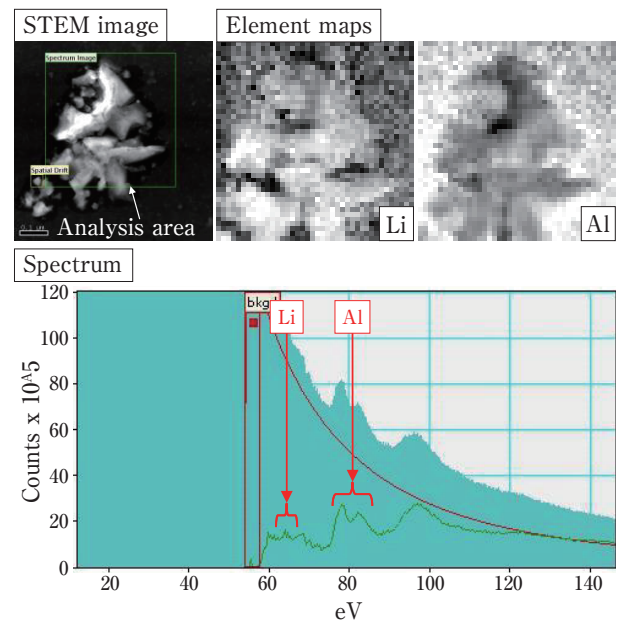


Fig. 10 TEM-EELS analysis of oxide film on the filler alloy after brazing No.3 material.

Table 2 Free energies of formation for reactions of Mg or Li with Al_2O_3 .

No.	Reactions	ΔG (kJ) at 600°C	Remarks
1	$Mg + 1/3Al_2O_3 \rightarrow MgO + 2/3Al$	-45.1	
2	$Mg + 4/3Al_2O_3 \rightarrow MgAl_2O_4 + 2/3Al$	-73.9	complex oxide
3	$2Li + 1/3Al_2O_3 \rightarrow Li_2O + 2/3Al$	-17.7	
4	$Li + 2/3Al_2O_3 \rightarrow LiAlO_2 + 1/3Al$	-69.9 (at 500°C)	complex oxide

the free energies of formation are negative, the free energy of formation of either complex oxide with aluminum is more negative than formation of a single oxide such as MgO or Li_2O . Therefore a reaction to form a complex oxide occurs thermodynamically. This corresponds with the result that the particles observed in this study were a complex oxide with aluminum.

3.4 Mechanism of oxide film destruction

From the results of this study, the mechanism of oxide film destruction in flux-free brazing is thought to proceed as follows. Although the oxide film exists over the entire surface of the filler alloy before brazing, it reacts with magnesium or lithium during brazing and is broken into complex oxide particles by that reaction. Then, the molten filler alloy is exposed between the oxide particles. As a consequence, brazing is possible.

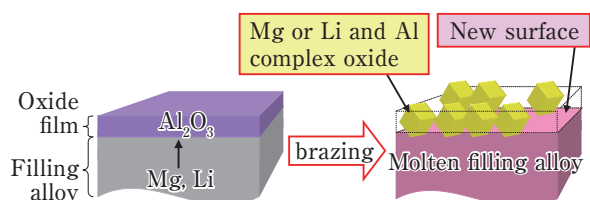


Fig. 11 Postulated mechanism of the oxide film destruction in flux-free brazing.

4. Conclusion

Flux-free brazing of aluminum is possible by the use of magnesium or lithium. It is effective to add magnesium to the core alloy than to the filler alloy. Lithium is a preferred element for improving the flux-free brazeability over magnesium. A brazing sheet containing 0.02% lithium in the filler alloy had a brazeability approaching that in the CAB method.

The mechanism of oxide film destruction is thought to be as follows. The additive element (magnesium, lithium) that diffused to the surface during brazing reacts with the oxide film (Al_2O_3) to form complex oxide particles with aluminum. As a result, the oxide film is broken into fine particles of 200 nm or less in size, and a new surface of filler alloy is exposed between the particles. Finally, a fillet is formed.

REFERENCES

- 1) W. Schultze and H. Schoer: *Welding Journal*, **52** (1973), October, 644.
- 2) A. Wittebrood, A. Burger and S. Kirakham: *VTMS*, **10** (2011), 35.
- 3) EP2835211: UACJ Corporation (2014).



Tomoki Yamayoshi
Research Department V,
Research & Development Division,
UACJ Corporation



Yasunaga Itoh
Research Department VII,
Research & Development Division,
UACJ Corporation



Atsushi Fukumoto
Research Department IV,
Research and Development Division,
UACJ Corporation